Pergamon

Int. J. Heat Mass Transfer. Vol. 38, No. 17, pp. 3149–3159, 1995

0017–9310/95 $9.50+0.00

0017–9310(95)00066–6

Heat transfer and fluid flow of natural convection adjacent to upward-facing horizontal plates

KENZO KITAMURA and FUMIYOSHI KIMURA

Department of Energy Engineering, Toyohashi University of Technology, Tempaku-cho, Toyohashi 441, Japan

(*Received* 9 *August* 1994 *and in final form* 3 *February* 1995)

Abstract—Natural convective flows over upward-facing horizontal plates were investigated experimentally. The main concerns were the fluid flow and local heat transfer characteristics over a wide range of modified Rayleigh numbers from 10^6 to 10^{15}. Test plates 20–1500 mm wide were utilized to attain such Rayleigh numbers and they were heated with uniform heat fluxes. The test fluid was water. The fluid flows over the plates and the surface temperatures of the plates were visualized with dye and by liquid crystal thermometry respectively. Extensive measurements of the local heat transfer coefficients were also carried out. The result from the wide plates showed that the following four regions appear over the plates at a streamwise distance x from the leading edge: (1) a laminar boundary layer region, (2) a streaky, transitional flow region, (3) a turbulent region and (4) a collision region. In particular, the second region covers a considerable portion of the total surface, and the local heat transfer coefficients there decrease proportionately with x. Thus, it was found that the width of the plates exerts a serious influence on the average heat transfer coefficients even at the highest Rayleigh numbers of the present experiments.

1. INTRODUCTION

Although natural convective flows over horizontal, heated surfaces appear in a wide variety of industrial equipment as well as in many natural circumstances, they have not been as extensively studied as flows adjacent to vertical surfaces. This is mainly due to the fact that the flows adjacent to horizontal surfaces are complicated and easily become three-dimensional when the plates are of practical sizes. This has hampered analytical treatments. Therefore, in order to obtain basic information on the flow and heat transfer of natural convection, experimental investigations are necessary.

Table 1 shows previous heat transfer experiments carried out with horizontal plates of square or rectangular plan-forms. Isothermal test plates were utilized in most of these experiments. The table summarizes the sizes of the test plates, experimental ranges of Rayleigh numbers which are based on the width of the plates, measured quantities together with the measurement techniques, principal results and other relevant experimental conditions. Among these experiments, the work by Fishenden and Saunders [1] may be the first that correlated the overall heat transfer coefficients of the horizontal plates with the form:

$$Nu = C\,Ra^n \tag{1}$$

They determined empirically the following sets of coefficients C and exponents n of the equation as: $C = 0.54$, $n = 1/4$ and $C = 0.14$, $n = 1/3$ for the laminar and turbulent flows respectively. Thereafter, several workers [2–5] measured the overall heat transfer coefficients of plates with different sizes and plan-forms using various techniques. Although some workers listed in the table focused their main concerns on inclined plates rather than horizontal plates, they all proposed the coefficients C and the exponents n for horizontal plates. It is obvious from the table that all of the previous workers have classified the flows simply into laminar and turbulent flows based on the Rayleigh numbers of the plates. Then, they recommended different sets of coefficients and exponents for each flow. These results are helpful for estimating the overall heat transfer under prescribed surface conditions. However, they give little insight into the flow and temperature fields over the plates.

Meanwhile, the visualization study by Husar and Sparrow [6] may be the first work that dealt with the flow field over horizontal heated surfaces. An electrochemical technique was used to visualize the flow field. They observed that the flows move along parallel paths over the plate and reach the central region of the plate, yet, the reasons for such flow paths were not discussed in detail. Rotem and Claassen [7] carried out the visualization experiments for air using a semi-focusing Schlieren apparatus. They reported that laminar boundary layers exist near the plate edges and then break down into irregular convection patterns some distance from the edges. Pera and Gebhart [8, 9] measured the temperature distribution and the local heat transfer coefficients of the laminar boundary layer flows of air by using a Mach–Zender interferometer. They revealed that the laminar boundary

NOMENCLATURE

A	surface area
C	constant
g	gravitational acceleration
Gr	Grashof number, $g\beta\Delta TW^3/\nu^2$
Gr^*	modified Grashof number, $g\beta q_w W^4/\kappa\nu^2$
Gr_x^*	local modified Grashof number, $g\beta q_w x^4/\kappa\nu^2$
h_m	average heat transfer coefficient, $q_w/(T_{wm}-T_\infty)$
h_x	local heat transfer coefficient, $q_w/(T_{wx}-T_\infty)$
L	span of test plate
n	exponent
Nu	average Nusselt number, $h_m W/\kappa$
Nu_x	local Nusselt number, $h_x x/\kappa$
Pr	Prandtl number
q_w	wall heat flux
Ra	Rayleigh number, $Gr\,Pr$
Ra^*	modified Rayleigh number, Gr^*Pr
Ra_x^*	local modified Rayleigh number, Gr_x^*Pr
s	distance from leading edge to onset of separation
T	temperature
W	width of plate
x	distance from leading edge.

Greek symbols

β	coefficient of volume expansion
κ	thermal conductivity of fluid
λ	spanwise spacing between streaks
ν	kinematic viscosity of fluid.

Subscripts

m	average
w	wall
x	at location x
∞	at environment.

layers begin to separate when the value of $Gr_x^{1/3}$ exceeds 80. Ishiguro *et al.* [10] carried out the visualization experiments also by means of a Mach–Zender interferometry. They reported that the temperature fields over the plate become three-dimensional when the Rayleigh numbers based on the plate width exceed 10^5.

Reviewing these experiments on flow and temperature fields over plates, laminar boundary layer flows in the vicinity of leading edges have been the main subject of previous investigations. Contrary to this, very little interest has been directed towards flow and temperature fields in the downstream region of boundary layers, where flow separation and transition to turbulence take place. Pera and Gebhart [9] reported by means of smoke tests that the separation occurs three-dimensionally; still, the mechanisms of such separation remain unclear. The transition to turbulence is another subject that has not been fully investigated. The flow separation and the turbulent transition exert serious influences on the local heat transfer. Although Ishiguro *et al.* [10] and Yousef *et al.* [11] have measured the local heat transfer coefficients in the downstream region of the separation, their results afford limited information on the correlation between the flow fields and the local heat transfer characteristics.

Considering the above, the present authors carried out extensive visualization experiments first on the flow and temperature fields in order to obtain a comprehensive picture of the natural convections adjacent to the horizontal plates. The flows over the plate and the surface temperatures of the plate were visualized with dye and by liquid crystal thermometry respectively. For convenience, water was used as a test fluid and the test plates were heated with uniform heat fluxes. Next, the local heat transfer coefficients were measured under the same experimental conditions as above: this was in order to investigate the correlation between the flow field and the local heat transfer. The width of the test plate was varied from 20 to 1500 mm to enable experiments in extremely wide ranges of the modified Rayleigh numbers from 10^6 to 10^{15}. Although it is difficult to compare the modified Rayleigh numbers of the present uniform heat flux plates directly with the Rayleigh numbers of previous isothermal plates, the maximum Rayleigh numbers of the present plates are estimated as two or three orders of magnitude larger than those of previous plates. The present results will, therefore, provide practical information on the local as well as the overall heat transfer coefficients for large plates.

2. EXPERIMENTAL APPARATUS AND MEASUREMENTS

The present apparatus is schematically illustrated in Fig. 1. The apparatus shown in Fig. 1(a) and (b) was utilized for experiments with smaller test plates, whose width was less than 250 mm, and for larger test plates with widths of 850 and 1500 mm. All the test plates consisted of acrylic resin plates 10 mm thick and stainless steel foil heaters 30 μm thick. The heaters were glued on the surfaces of the acrylic plates and were connected in series. A uniform heat flux condition was realized by supplying AC power to these heaters. The back of the plate was insulated thermally with 10 mm thick Styrofoam insulation. The width of the test plates, W, was varied from 20 to 1500 mm. In order to inhibit the side flows and to realize a two-

Table 1. Previous heat transfer experiments for horizontal surfaces

Reference	Fluid	Test plate dimensions $W \times L$ in cm^2	Collar†/ Fence	Range of Ra numbers	Measured quantities (technique)	Heat transfer correlations
Fishenden and Saunders [1] (1957)	air	max. 60×60 (square)	none	$10^5 < Ra < 3 \times 10^{10}$	average heat transfer coefficient (?)	laminar: $10^5 < Ra < 2 \times 10^7$ $Nu = 0.54\ Ra^{1/4}$ turbulent: $2 \times 10^7 < Ra < 3 \times 10^{10}$ $Nu = 0.14\ Ra^{1/3}$
Hassan and Mohamed [2] (1970)	air	20×50.4	none	$1.1 \times 10^3 < Gr < 3 \times 10^8$	average heat transfer coefficient (heat flux meter)	$Nu = 0.12\ Gr^{1/3}$
Fujii and Imura [3] (1972)	water	5×10 30×15	fence	$7 \times 10^6 < Ra < 2 \times 10^8$ $5 \times 10^8 < Ra < 6 \times 10^{10}$	average heat transfer coefficient (thermocouples)	$Nu = 0.16\ Ra^{1/3}$ $Nu = 0.13\ Ra^{1/3}$
Goldstein *et al.* [4] (1973)	air	$W = 2.03$–5.84 aspect ratio = 7	none	$2.8 \times 10^2 < Ra < 9 \times 10^3$	average mass transfer coefficient (naphthalene sublimation)	$Sh = 0.59\ Ra^{1/4}$ ($Sc = 2.5$)
Al-Arabi and El-Riedy [5] (1976)	air	$15 \times (25$–$60)$	none	$2 \times 10^5 < Ra < 10^9$	average heat transfer coefficient (amount of condensate)	laminar: $2 \times 10^5 < Ra < 4 \times 10^7$ $Nu = 0.70\ Ra^{1/4}$ turbulent: $4 \times 10^7 < Ra < 10^9$ $Nu = 0.155\ Ra^{1/3}$
Ishiguro *et al.* [10] (1977)	water	0.76×8 2.8×13 20.5×17	collar collar collar + fence	$3 \times 10^5 < Ra < 10^{10}$	average heat transfer coefficient local heat transfer coefficient visualization	$Nu = 0.20\ Ra^{1/3}$
Yousef *et al.* [11] (1982)	air	10×10 20×20 40×40 (square)	collar collar collar	$1.9 \times 10^6 < Ra < 1.7 \times 10^8$	average heat transfer coefficient local heat transfer coefficient fluid temp. (Mach-Zender)	laminar: $3 \times 10^6 < Ra < 4 \times 10^7$ $Nu = 0.622\ Ra^{1/4}$ turbulent: $4 \times 10^7 < Ra < 1.7 \times 10^8$ $Nu = 0.162\ Ra^{1/3}$

† collar stands for the insulated extension plate upstream of the test plate.

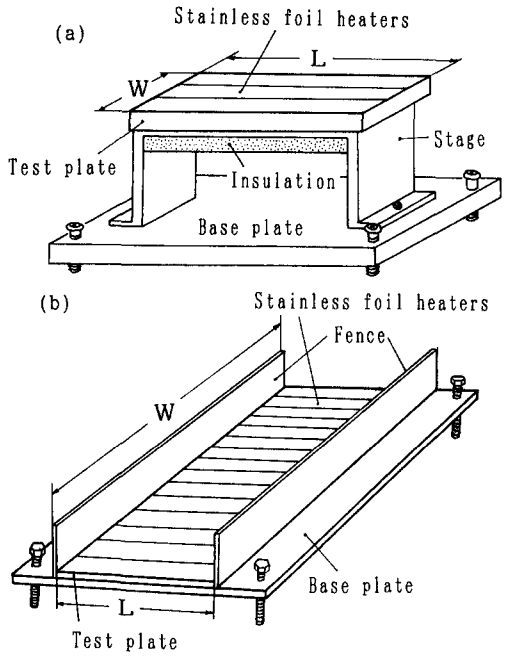

Fig. 1. Experimental apparatus.

dimensional flow field over the plates, the aspect ratio of the plate, span/width, was kept at three for the smaller test plates. It was, however, difficult to attain such a high aspect ratio for the 850 and 1500 mm wide plates due to the limited volume of the water tanks. Thus, fences 250 mm high were installed on the both sides of the larger test plates to inhibit the side flows. The span of the larger test plates was kept at 500 mm.

Surface temperatures of the heat transfer plates, T_{wx}, were measured with Chromel–Alumel thermocouples of 70 μm diameter, which were spot-welded on the back of the heaters along the streamwise direction of the plates. The temperatures of the ambient fluid, T_∞, were also measured with thermocouples of the same material and diameter as above, placed 50 mm apart from the plate edge and in the same horizontal plane as the plate surface. The heat loss by conduction from the heaters to the back of the test plates was estimated as less than 4% of the total heat generation on the heaters. Thus, the surface heat fluxes, q_w, were calculated from the electric power to the heaters, Q, and the total surface area of the plates, A, as: $q_w = Q/A$. By using the temperatures, T_{wx}, T_∞, and the heat flux, q_w, the local heat transfer coefficients, h_x, were calculated as: $h_x = q_w/(T_{wx} - T_\infty)$.

In order to minimize the effects of thermal property variations on the heat transfer, temperature differences between the surface and the ambient fluid were maintained as less than 10 K throughout the experiments. Thermophysical properties in non-dimensional parameters were estimated at the film temperatures as: $T_f = (T_w + T_\infty)/2$.

The above apparatus was placed horizontally on the bottom of rectangular water tanks using screws to adjust the levels. Tanks of 750×750 mm^2 cross-sectional area and 700 mm deep and 1000×2000 mm^2 cross-sectional area and 1000 mm deep were utilized for the experiments with the smaller and the larger test plates, respectively.

3. RESULTS AND DISCUSSION

3.1. *Visualizations of flow and temperature fields*

The surface temperatures of the test plates were visualized by means of liquid crystal thermometry. The aims of the experiments were to obtain comprehensive information not only on the temperature fields over the plates but also on the local heat transfer from the plates. Figure 2 shows the visualized surface temperatures for the test plates with various widths. These photos were taken from directly above the plates. Before discussing the results, some explanations will be needed to interpret these photos. The liquid crystal sheets utilized here change color from dark red to blue with increasing temperatures from 29°C to 34°C. The colors yellow and green show the intermediate temperatures. These photos also represent the distributions of the local heat transfer coefficients, because the test plates were heated with uniform heat flux and the temperature of the ambient fluid was kept constant. Thus, the regions of high (blue) and low (dark red or brown) temperatures correspond to those of the low and high heat transfer coefficients respectively. Moreover, we will find vertical lines in Figs. 2(c) to (g), which are yellow or brown in color. However, it should be noted that these lines represent the dividing lines of the heater strips.

Figure 2(a) depicts the result for the plate 20 mm wide. The temperatures are almost uniform in the spanwise direction parallel to the plate edges, while they vary significantly towards the streamwise direction and become higher with distance from the plate edges. The result implies that the heat transfer coefficients are highest at the leading edges of the plate and decrease proportionately with distance. Similar temperature variations are also observed with the plate 30 mm wide, except in the central portion of the plate, where low-temperature spots appear as shown in Fig. 2(b). These spots are generated periodically at regular intervals from 3 to 5 seconds. Meanwhile, the spots become stationary and increase in number for the 50 mm wide plate as shown in Fig. 2(c). These spots are, then, elongated to the streamwise direction and become streaky with further increase in plate width as demonstrated in Figs. 2(d) and (e). The low-temperature streaks occur at almost constant spanwise spacings and cover a considerable portion of the surfaces. We also observed that these patterns remain unchanged with time. In addition to this, different temperature patterns appear in the central portion of the 250 mm wide plate as shown in Fig. 2(f). Those patterns change irregularly with time and move as a whole to the center of the plate. Similar temperature

patterns are also obvious in Figs. 2(g) and (h) for the plates 850 and 1500 mm wide respectively. Meanwhile, we observe that somewhat different temperature patterns appear near the center of the plates, which are characterized by small and dense low-temperature streaks. The patterns move randomly but sway around the center of the plate.

Summarizing the above results, the following four distinct temperature patterns are obvious on the surfaces. These are: (i) two-dimensional patterns in the vicinity of the leading edges, (ii) steady and streaky patterns downstream from the patterns (i), (iii) unsteady and irregular patterns next to patterns (ii), and (iv) small and dense patterns near the centerline of the plate. Among these patterns, patterns (ii) and (iii) are of particular importance, because they occupy a major portion of the surface. Therefore, further visualization experiments were carried out on the flow fields to investigate the reasons for these patterns.

Typical examples of the visualized flow fields are shown in Fig. 3 with the case of a 150 mm wide plate. Uranine dissolved with water was utilized as a dye. In order to visualize the flow field two-dimensionally, a slit was installed at the leading edge and level to the plate surface. As shown in Fig. 3(a), dye issued slowly from the slit flows along the plate and, then, separated from the surface some distance from the leading edge. Figure 3(b), taken from directly above the plate, demonstrates that the dye forks into many filaments when the separation takes place and that these filaments are arranged at almost constant spacings. The filaments then begin to fluctuate and gather slowly to the central region of the plate, where they change direction vertically and ascend away from the plate. Meanwhile, when another dye is injected from a small stainless steel pipe placed 4 mm above the plate, the dye descends to the pocket between the above filaments and attaches to the surface as shown in Fig. 3(c). Taking account of the fact that the dye represents the movement of the low-temperature fluid above the plate, the attachment of the low-temperature fluid will result in streaky low-temperature patterns. The combined visualizations with dye and liquid crystal sheet also confirmed this. Furthermore, it is apparent from these photos that laminar boundary layers exist near the leading edges and two-dimensional temperature patterns are generated in this region.

Similar flow visualization experiments were performed with a plate 850 mm wide and the results are presented in Fig. 4. The dye issued from the leading edge attaches to the surface for a short distance and separates three-dimensionally. The dye filaments are then distorted and fluctuate irregularly. This behaviour implies that the flow undergoes turbulent transition. Then, the fluctuations are amplified significantly and, finally, a fully turbulent state is achieved in the far downstream region of the plate. The figure also demonstrates that the turbulent flows coming from both edges collide with each other in the central region of the plate and they ascend away from the plate. The result indicates that main flows of natural convection exist over the large plates. Meanwhile, it has been recognized in general that the turbulent cellular convections characterized by thermals or plumes are dominant in the downstream regions of the separation and that the main flows will not exist. Taking account of this, the present result is noteworthy. Moreover, comparisons were made between these results and those of the surface temperature visualizations. The result confirms that irregular and unsteady temperature patterns are generated by turbulent fluid motion, and also that small and dense temperature patterns in the central region of the plate result from collision of flows.

Summarizing the above, the following specific flows became apparent over large plates. These are: (v) laminar boundary layer flows in the vicinity of the plate, (vi) transitional flows characterized by three-dimensional separations and steady and streaky temperature patterns, (vii) turbulent flows and (viii) colliding flows in the central region of the plate. Among these flows, the transitional flows are of particular importance, because the flows cover a considerable portion of the total surface. However, very little information is available on these flows.

Further investigations were, therefore, made on the transitional flows in the present study. What characterizes the flows are the separation phenomena, so the onset of the separation was investigated first. Although it is difficult to determine the onset precisely because of the complexity of the three-dimensional separation, the location where the dyes begin to detach from the plate was defined here as the onset of separation. The location also corresponds to the beginning of the low-temperature streaks. The distances, s, from the leading edge to the onset were measured and averaged under the various conditions of the plate sizes and of surface heat fluxes. The results are plotted in terms of the surface heat fluxes and are shown in Fig. 5. The separation occurs 10–20 mm downstream from the leading edge and the values become smaller with heat flux. On the other hand, the width of the plate exerts little influence on the onset of the separation.

The next concerns were directed to the three-dimensional separation. The length scale that characterizes the separation is the spanwise spacings, λ, of the dye filaments or of the low-temperature streaks. We found that the spacings obtained from the dye filaments and from the streaks coincide with each other. The results are shown in Fig. 6. The mean spanwise spacings between the dye filaments are of the order of several millimeters. The spacings become smaller with increasing wall heat fluxes, yet, they are independent of the width of the plates.

Several efforts were made to obtain non-dimensional correlations for the onset and also for the mean spacings of the separation by using the above data, but the results were unsatisfactory. This is probably due to the marked variations in the surface temperatures in the streamwise direction. However, it was

found that the modified Rayleigh numbers, Ra_s^*, based on the distance s, gather within the range of $1.5 \times 10^6 < Ra_s^* < 4 \times 10^6$, and also that the values become smaller with an increase in surface heat flux. Moreover, the modified Rayleigh numbers, Ra_λ^*, for which the characteristic lengths are the mean spanwise spacings, λ, fall within the narrow range of $1.0 \times 10^5 < Ra_\lambda^* < 1.5 \times 10^5$. The numbers become larger with heat flux.

3.2. *Local heat transfer characteristics*

Taking account of the above results, we subsequently carried out the measurements on the local heat transfer coefficients using thermocouples. The problem arises as for the local heat transfer measurements, in particular, in the transitional region, because the low-temperature streaks appear there and their location remains unchanged with time. The occurrence of such streaks will lead to marked spanwise variations in the coefficients. Therefore, the coefficients from this region were defined as the values averaged in the spanwise direction. In spite of the definition, it is still difficult to determine the coefficients precisely from the output of the thermocouples, because the spanwise spacings of the streaks are of the orders of several millimeters and we cannot place thermocouples at intervals small enough to detect the spanwise variations.

Meanwhile, we observed that these streaks change their location during a run conducted under the same experimental conditions. Making use of this fact, we repeated the measurements of the surface temperatures at least 20–30 times under the same experimental conditions. The thermocouples were placed symmetrically with respect to the centerline of the plates, so that more than 40–60 data were collected to yield the local heat transfer coefficients. An error analysis was performed on these data. The results indicated that the above numbers are large enough to calculate the mean values and that the deviations of the calculated coefficients against the real coefficients are estimated as less than $\pm 3\%$ at 95% coverage.

The local heat transfer coefficients thus obtained are shown in Fig. 7 with the case of $q_w = 3000\ \mathrm{W\ m^{-2}}$. The results for the plates less than 250 mm wide are plotted in terms of the distance x. The spanwise variations of the local coefficients in the transitional region are also represented with bars in the figure. The highest coefficients are realized at the leading edge, and the coefficients decrease rapidly with x and reach a minima at about $x = 10$ mm. Then they turn to increase and show a maxima at about $x = 20$ mm. In the downstream region of the maxima, the heat transfer coefficients decrease gradually with x. The occurrence of the above minimum and maximum coefficients is worth noting, because no previous worker has reported such minimum and maximum coefficients.

Similar variations in the local heat transfer coefficients are also observed with the larger test plates, as shown in Fig. 8. Here, the data from plates 850 and 1500 mm wide are plotted in terms of the distance x together with the data for the 250 mm wide plate for reference. The minimum and maximum coefficients occur near the leading edge. The figure also reveals that the local heat transfer coefficients decrease gradually from maxima at around $x = 20$ mm to those at around $x = 300$ mm. A few workers have measured the local heat transfer coefficients from the large plates, yet, the above variations of the maximum coefficients have not been reported. The result implies that local heat transfer coefficients still depend on the location x even in the region far downstream from the separation. Moreover, in the downstream region of the above, the coefficients for the 850 mm wide plate increase slightly towards the centerline of the plate, while they remain almost constant for the 1500 mm wide plate.

The present results on the heat transfer were next compared with those of surface temperature visualizations. The comparisons are intended not only to confirm the present heat transfer variations but also to investigate the relation between the temperature field and the local heat transfer. The following relations were found between the above two: (1) a marked decrease in heat transfer coefficients near the leading edge occurs in the laminar boundary layer region, (2) minimum coefficients appear just upstream of the separation, (3) maximum coefficients correspond to the location where the low-temperature streaks spread widest in the spanwise direction, (4) a gradual decrease in the coefficients after the maxima occurs in the region where the low-temperature streaks become narrower and more obscure, (5) uniform coefficients are obtained in the turbulent flow region and (6) a slight increase in the coefficients occurs in the central region of the plate where the turbulent flows collide with each other. In particular, the last result suggests that the collision of the main flows yields higher coefficients than those of the turbulent regions. Moreover, these results well explain the present variations in the local coefficients.

It is also obvious from Figs. 7 and 8 that the present heat transfer data from the different plates gather around a single curve with few exceptions and that the exceptions are all concerned with the data from the collision regions where higher heat transfer coefficients were obtained. The result demonstrates that the width of the plate exerts little influence on the distributions of the local heat transfer coefficients except in the collision region. Making use of this, all the present heat transfer data except those from the collision region were replotted in the local Nusselt number–local modified Rayleigh number plane as shown in Fig. 9. The lower and the upper plots in the figure represent the results for the 1500 mm wide plate and for the plates 20–850 mm wide, respectively. The two data plots gather around a single curve, and the curve changes its gradient in the specific ranges of the modified Rayleigh numbers.

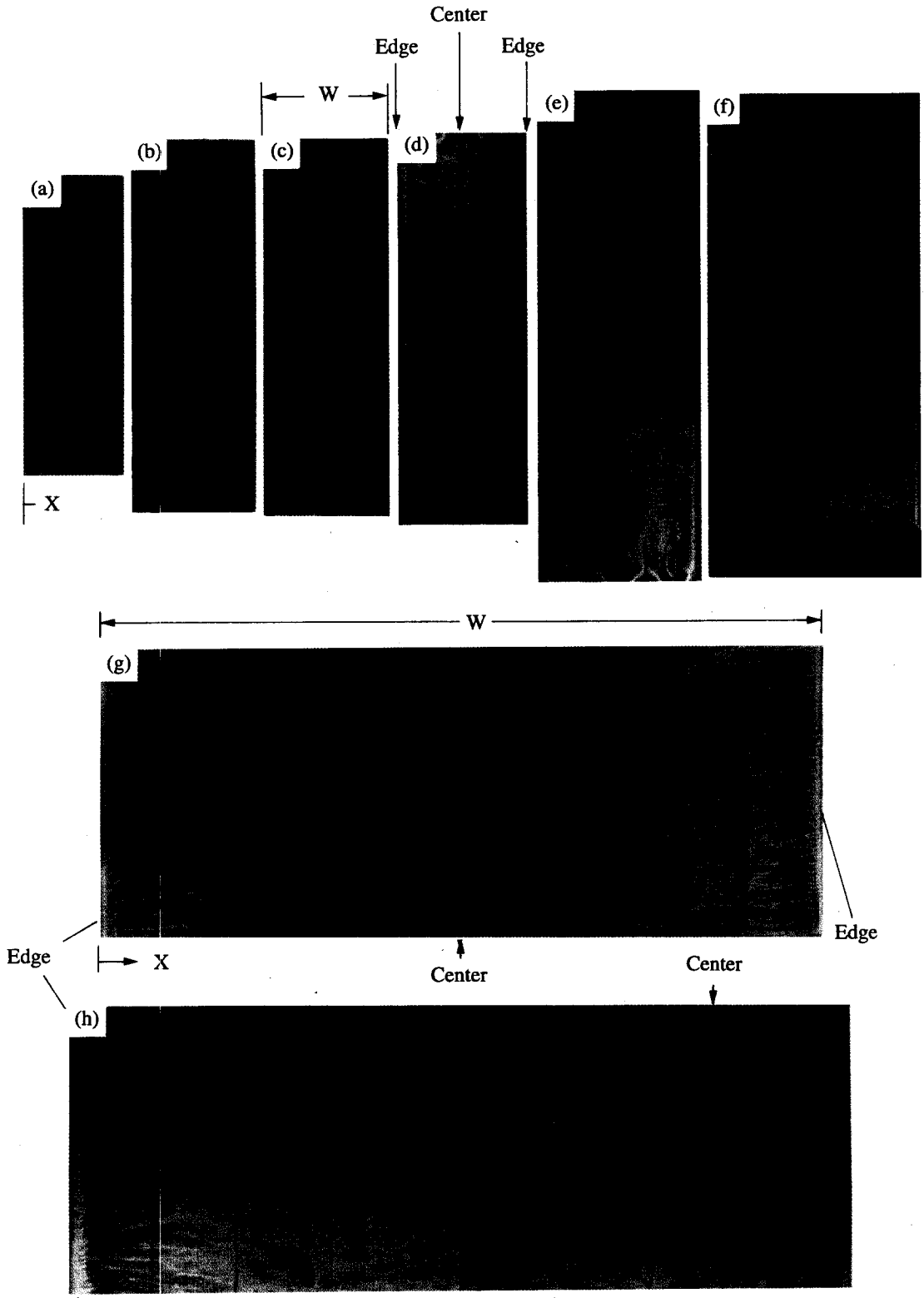

Fig. 2. Visualized surface temperature distributions of test plates. (a) $W = 20$ mm, $Ra^* = 8.2 \times 10^6$, (b) $W = 30$ mm, $Ra^* = 3.1 \times 10^7$, (c) $W = 50$ mm, $Ra^* = 5.5 \times 10^8$, (d) $W = 100$ mm, $Ra^* = 5.9 \times 10^9$, (e) $W = 150$ mm, $Ra^* = 3.9 \times 10^{10}$, (f) $W = 250$ mm, $Ra^* = 3.1 \times 10^{11}$, (g) $W = 850$ mm, $Ra^* = 4.3 \times 10^{13}$, (h) $W = 1500$ mm, $Ra^* = 4.3 \times 10^{14}$.

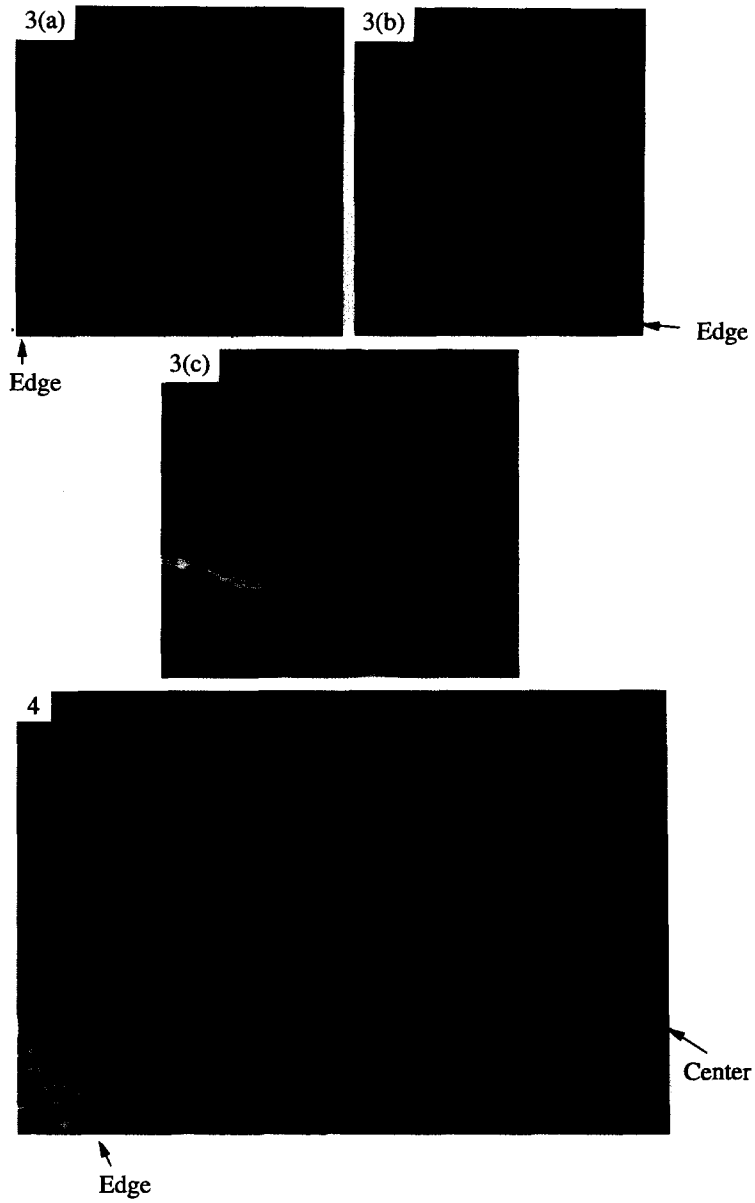

Fig. 3. Visualized flow fields over a 150 mm wide plate. (a) Side view, (b) front view, (c) side view.
Fig. 4. Visualized flow fields over an 850 mm wide plate.

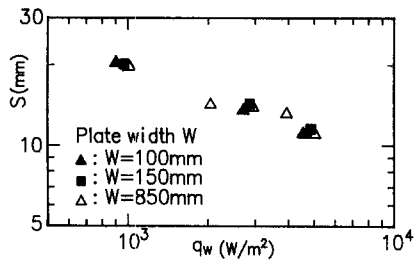

Fig. 5. Mean distances from the leading edge to the onset of separation.

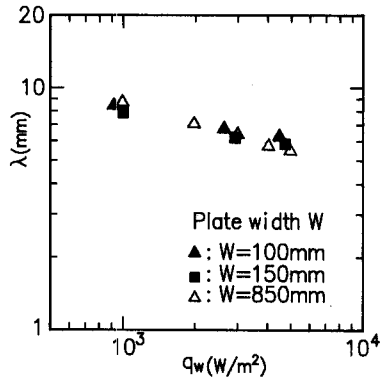

Fig. 6. Mean spanwise spacings between dye filaments.

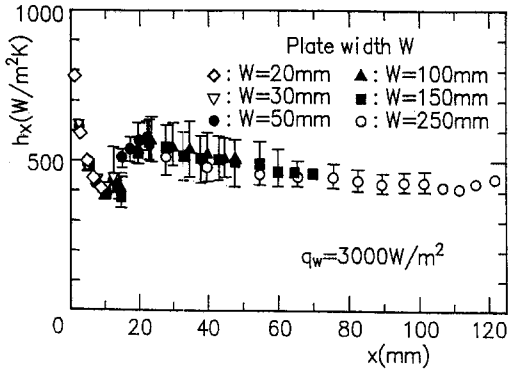

Fig. 7. Local heat transfer coefficients for smaller plates.

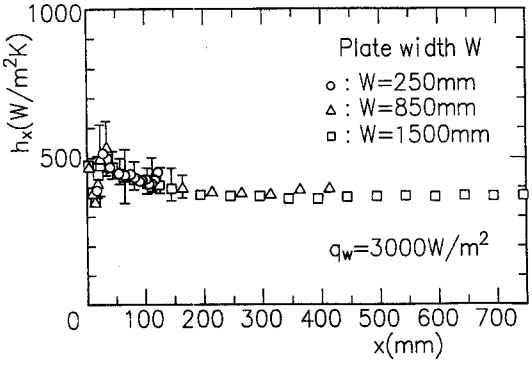

Fig. 8. Local heat transfer coefficients for larger plates.

Assuming the following relation between the local Nusselt and modified Rayleigh numbers:

$$Nu_x = C\,Ra_x^{*1/n}. \tag{2}$$

The gradients $1/n$ and the coefficients C were determined for each region of the modified Rayleigh numbers. It was revealed that the following equations express the present curve fairly well:

Region (I); $10^2 < Ra_x^* < 10^6$

$$Nu_x = 0.66 Ra_x^{*1/6} \tag{3}$$

Region (II); $10^6 < Ra_x^* < 5\times 10^7$

$$Nu_x = 0.066 Ra_x^{*1/3} \tag{4}$$

Region (III); $5\times 10^7 < Ra_x^* < 8\times 10^{10}$

$$Nu_x = 0.70 Ra_x^{*1/5} \tag{5}$$

Region (IV); $8\times 10^{10} < Ra_x^* < 10^{14}$

$$Nu_x = 0.20 Ra_x^{*1/4}. \tag{6}$$

Although the maximum and minimum Rayleigh numbers for each region (I)–(IV) are somewhat arbitrary and cannot be determined strictly, the following relation was found from the above numbers: (1) Region (I) can be referred to as the laminar flow region, (2) Region (II) corresponds to the transitional region from the minimum to maximum coefficients, (3) Region (III) corresponds also to the transitional region after the maximum coefficients, and (4) Region (IV) can be termed as the turbulent flow region, where the local heat transfer coefficients are uniform and independent of x.

3.3. *Average heat transfer characteristics*

In general, the average heat transfer coefficients, h_m, are defined as the integral average of the local heat transfer coefficients, h_x, over the entire plate width, W.

$$h_m = \frac{1}{W}\int_0^W h_x\,dx. \tag{7}$$

Based on the above definition, we calculated the average coefficients by introducing the local coefficients obtained from equations (3)–(6) into equation (7). The coefficients thus obtained were then normalized with the plate width to yield the average Nusselt numbers, Nu. The results become as follows:

Region (I); $1.6\times 10^3 < Ra^* < 1.6\times 10^7$

$$Nu = 1.25 Ra^{*1/6} \tag{8}$$

Region (II); $1.6\times 10^7 < Ra^* < 8\times 10^8$

$$Nu = 0.04 Ra^{*1/3} + 9.7 \tag{9}$$

Region (III); $8\times 10^8 < Ra^* < 1.3\times 10^{12}$

$$Nu = Ra^{*1/5} - 13.5 \tag{10}$$

Region (IV); $1.3\times 10^{12} < Ra^* < 1.6\times 10^{15}$

$$Nu = 0.20 Ra^{*1/4} + 37. \tag{11}$$

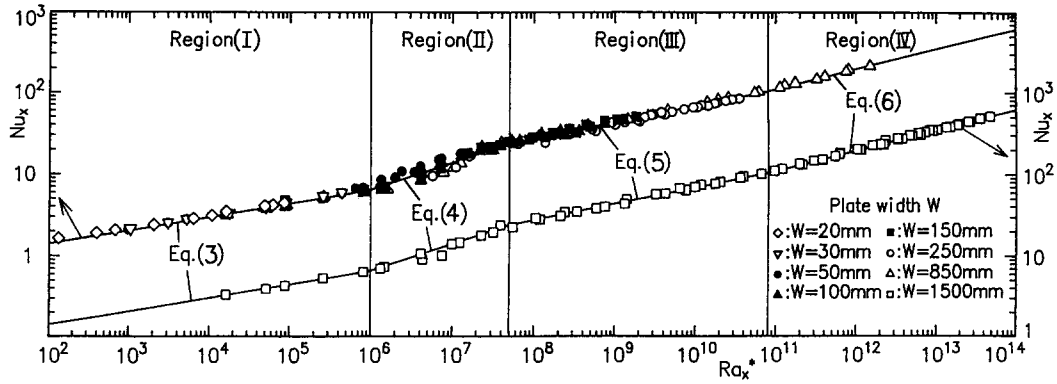

Fig. 9. Local Nusselt numbers vs local modified Rayleigh numbers.

The modified Rayleigh numbers, Ra^*, in the above equations are based on the width of the plates. Equations (8)–(11) are shown with the solid lines in Fig. 10. Meanwhile, we also calculated the average Nusselt numbers by introducing the measured local coefficients directly into equation (7). The results are shown with symbols in the figure. The Nusselt numbers estimated from equations (8)–(11) coincide fairly well with those calculated from the direct measurements. The result implies that the increment in the heat transfer coefficients due to the flow collision is small and contributes little to the overall heat transfer. Thus, the average Nusselt numbers of the present plates can be correlated well with equations (8)–(11).

Among these equations, equation (11) is of particular importance, because the equation demonstrates that the average heat transfer coefficients still depend on the plate width even at Rayleigh numbers up to 10^{15}. Meanwhile, several previous workers have measured the average heat transfer coefficients from large, isothermal plates and proposed the empirical correlations as listed in Table 1. In order to compare the present equations for the uniform heat flux plates with previous equations for the isothermal plates, the latter equations were transformed using the relation $Gr^* = Gr\,Nu$. The results are shown also with lines in Fig. 10. The Nusselt numbers estimated from the previous equations seem to be in fairly good agreement with those from the present equations. However, it should be noted that the previous measurements have been carried out for ranges of the modified Rayleigh numbers less than 10^{12}, where transitional flows will be dominant over the plates, and, thus, the width of the plates will exert serious influence on the average heat transfer. Nevertheless, previous workers have proposed empirical equations with the form; $Nu \sim Ra^{1/3}$, which implies that the average heat transfer coefficients are independent of the plate width. Taking these facts into account, the previous equations are considered inaccurate from the physical point of view. This may be due partly to the presumption of previous workers that flows will become immediately turbulent in the downstream region of the separation and that turbulent flows will dominate over almost the entire surfaces. On the other hand, the present experiments revealed that a transitional

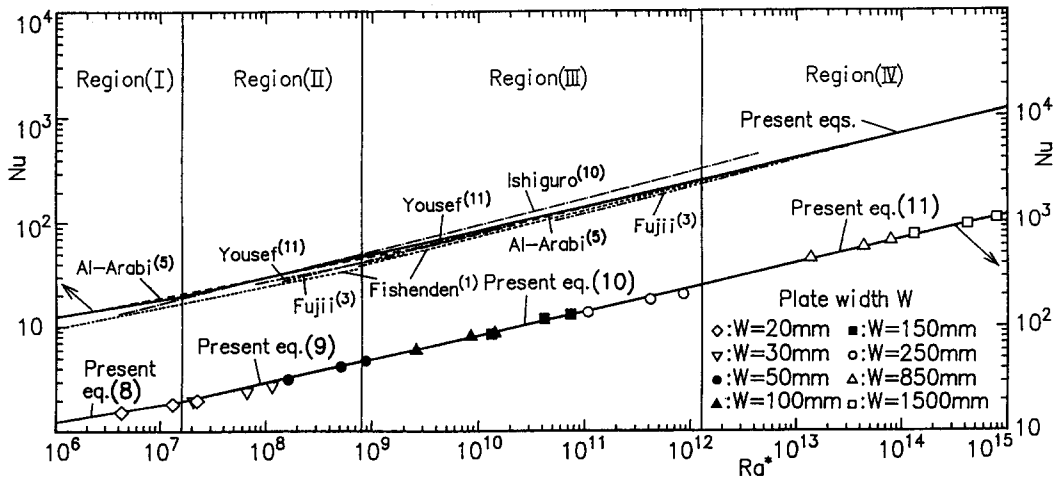

Fig. 10. Average Nusselt numbers vs modified Rayleigh numbers, correlation equations and comparisons with previous results.

region appears in between the laminar and turbulent regions and that the heat transfer from this region exerts serious influence on the overall heat transfer.

4. CONCLUSIONS

The fluid flow and the heat transfer of natural convections adjacent to horizontal plates were investigated experimentally in the present study. The flow and temperature fields over the plates were visualized first to obtain a comprehensive picture of natural convections over the plates. The measurements of the local heat transfer coefficients were subsequently carried out. The results were, then, compared with those from the visualization experiments to investigate the relation between the local heat transfer and the fluid flows over the plates. Water at room temperature was used as a test fluid. The rectangular test plates were heated with uniform heat flux. The width of the plates was varied from 20 to 1500 mm and this enabled experiments in an extremely wide range of modified Rayleigh numbers from 10^6 to 10^{15}. The maximum Rayleigh numbers of the present experiments are about two orders of magnitude higher than those of previous experiments. The following results were obtained from the visualization experiments.

(1) The surface temperatures of the test plates were visualized with liquid crystal thermometry and the following temperature patterns were found to appear over the plates with distance x from the leading edge: (i) two-dimensional patterns near the leading edges, (ii) steady and streaky low-temperature patterns, (iii) unsteady and irregular low-temperature patterns and (iv) small and dense low-temperature patterns.

(2) The flow visualization experiments revealed that the following flows appear over the plate: (v) laminar boundary layers near the leading edges, (vi) transitional flows which are characterized by the three-dimensional separation and by the attachment of the low-temperature fluid onto the surface downstream of the separation, (vii) fully turbulent flows and (viii) colliding flows near the centerline of the plates.

(3) The comparisons of the above two results revealed that the temperature patterns (i), (ii), (iii) and (iv) appear in the flow regions (v), (vi), (vii) and (viii) respectively.

Taking these results into account, the local heat transfer coefficients were measured along the streamwise direction x. The following results were obtained.

(4) The minimum and maximum coefficients appear at a location just upstream from the separation and at the location to which the ambient fluid attaches, respectively. The local heat transfer coefficients show significant variations even in the downstream region of the separation. Thus, the average heat transfer coefficients depend on the width of the plate even at the highest Rayleigh numbers of the present experiments. Furthermore, empirical correlations for the local and average Nusselt numbers were proposed based on these data.

Acknowledgement—The authors wish to acknowledge support from the Ministry of Education, Science and Culture of Japan through research grant no. 04650185.

REFERENCES

1. M. Fishenden and O. A. Saunders, *An Introduction to Heat Transfer*, p. 89, Clarendon Press, London (1957).
2. K. E. Hassan and S. A. Mohamed, Natural convection from isothermal flat surfaces, *Int. J. Heat Mass Transfer* **13,** 1873–1886 (1970).
3. T. Fujii and H. Imura, Natural convection heat transfer from a plate with arbitrary inclination, *Int. J. Heat Mass Transfer* **15,** 755–767 (1972).
4. R. J. Goldstein, E. M. Sparrow and D. C. Jones, Natural convection mass transfer adjacent to horizontal plates, *Int. J. Heat Mass Transfer* **16,** 1025–1035 (1973).
5. M. Al-Arabi and M. K. El-Riedy, Natural convection heat transfer from isothermal horizontal plates of different shapes, *Int. J. Heat Mass Transfer* **19,** 1399–1404 (1976).
6. R. B. Husar and E. M. Sparrow, Patterns of free convection flow adjacent to horizontal heated surfaces, *Int. J. Heat Mass Transfer* **11,** 1206–1208 (1968).
7. Z. Rotem and L. Claassen, Natural convection above unconfined horizontal surfaces, *J. Fluid Mech.* **38,** pt. 1, 173–192 (1969).
8. L. Pera and B. Gebhart, Natural convection boundary layer flow over horizontal and slightly inclined surfaces, *Int. J. Heat Mass Transfer* **16,** 1131–1146 (1973).
9. L. Pera and B. Gebhart, On the stability of natural convection boundary layer flow over horizontal and slightly inclined surfaces, *Int. J. Heat Mass Transfer* **16,** 1147–1163 (1973).
10. R. Ishiguro, T. Abe and H. Nagase, Natural convection over heated horizontal plates, *Trans. Jap. Soc. Mech. Engrs, Series B* **43,** (366), 638–645 (1977) (in Japanese).
11. W. W. Yousef, J. D. Tarasuk and W. J. Mckeen, Free convection heat transfer from upward-facing isothermal horizontal surfaces, *Trans. Am. Soc. Mech. Engrs, J. Heat Transfer* **104,** 493–500 (1982).